SIDEBAR 2.2: MONITORING GLOBAL DROUGHT USING THE SELF-CALIBRATING PALMER DROUGHT SEVERITY INDEX—

G. VAN DERSCHRIER, J. BARICHIVICH, I. HARRIS, P. D. JONES, AND T. J. OSBORN

Hydrological drought results from a period of abnormally low precipitation, sometimes exacerbated by additional evapotranspiration (ET), and its occurrence can be apparent in reduced river discharge, soil moisture, and/or groundwater storage, depending on season and duration of the event. Although drought could be identified in any of these variables, it is also commonly estimated using drought indices derived from meteorological observations because these records are often longer, more widespread, and more readily available.

Common drought indices (Trenberth et al. 2014) are derived solely from precipitation (Standardized Precipitation Index, SPI; Guttman 1999) or the difference between precipitation and potential ET (Standardized Precipitation Evapotranspiration Index, SPEI; Vicente-Serrano et al. 2010). Alternatively, an account of soil moisture can be kept to allow an estimate of actual ET to be used, together with precipitation, to obtain the Palmer Drought Severity Index (PDSI; Palmer 1965) and a variant called the self-calibrating PDSI (scPDSI; Wells et al. 2004). These are all relative indices, describing the severity of drought by comparison with the variations experienced during a reference period.

Recent studies using various drought indices have produced apparently conflicting results of how drought is changing under climate change (Trenberth et al. 2014). The discrepancies arise from different choices of drought index, precipitation dataset, and potential ET parameterization and the uncertainties therein. There is no consensus about which approach is most suitable. Here the physically based Penman–Monteith potential ET is used, instead of a potential ET estimate based only on air temperature, along with the scPDSI, which aims to be more comparable between diverse climate regions than the "traditional" PDSI (Wells et al. 2004). As with other indices, uncertainties in the input variables transfer through to the scPDSI. The baseline period, used to define and calibrate the scPDSI moisture categories, is the complete 1901–2014 period, making sure that "extreme" droughts (or pluvials) relate to events that do not occur more frequently than in approximately 2% of the months. This affects direct comparison with other hydrological cycle variables in Plate 2.1 which use a more recent climatology period.

Globally, the year 2014 was not particularly dry (compare Plate 2.1 hydrological cycle variables). The scPDSI metric (updated from van der Schrier et al. 2013a, using precipitation and potential ET from the CRU TS3.22 dataset of Harris et al. 2014) shows that only about 5% of the global land area saw severe (scPDSI < –3, Palmer 1965) drought conditions and about 1% saw extreme (scPDSI < –4) drought conditions (Fig. SB2.3). The area under drought, whether moderate, severe, or extreme, has decreased since the mid-1980s using this metric, and 2014 drought areas were smaller than the climatological average (for either the 1961–90 or 1981–2010 periods). However, this trend is not universal across all studies, depending especially on the precipitation dataset and the choice of reference period (Trenberth et al. 2014).

Despite the small global area experiencing drought in 2014, severe and extensive droughts occurred in some regions such as eastern Australia (Fig. SB2.4). This drought was still severe but has ameliorated in some places since 2013.

Parts of Central America (Guatemala, El Salvador, and Nicaragua) were in significant drought in 2014, with little change from 2013 (Fig. SB2.4). The remainder of Central America was very wet. Drought conditions were prevalent in tropical South America, particularly in coastal Peru, the western part of the Amazon basin, Uruguay, and parts of southern Brazil. Drought in the latter regions became much worse in 2014 and adverse impacts on surface water resources around São Paolo were widely reported in the media.

An extensive region with drought conditions was evident from Iran stretching into India. Dry conditions over India in 2014 were less severe than in 2013, while those over Pakistan became worse. Farther east in Asia,

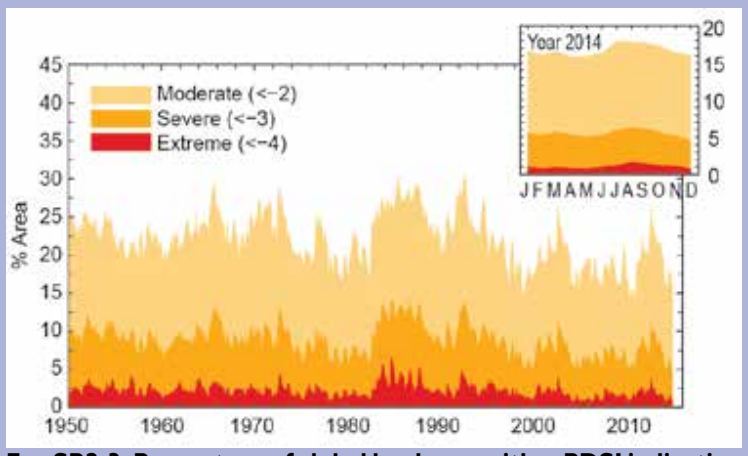

FIG. SB2.3. Percentage of global land area with scPDSI indicating moderate (< –2), severe (< –3) and extreme (< –4) drought for each month for 1950–2014. Inset: each month of 2014.

the scPDSI indicated the development of a moderate or severe drought in southeastern China in 2014.

Approximately 20% of southern Africa (below 12°S) experienced moderate drought, with more severe drought in localized areas such as South Africa and Madagascar. This area is slowly recovering from a dry spell that began in 2010; since that time the area with extremely dry conditions has steadily decreased. A large area in central Africa between Lake Chad and the equator also had prominent drought conditions, appearing more severe than the situation in 2013.

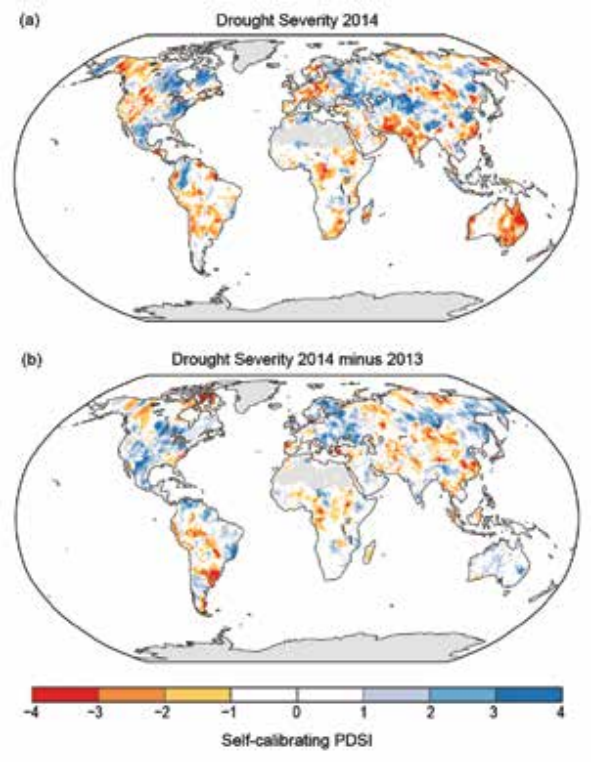

Drought conditions in parts of western North America have eased since July 2012 when nearly half of the region was under moderate drought conditions. This view of western North American drought is less extreme than that indicated by the U.S. Drought Monitor (http://droughtmonitor.unl.edu), which indicated extreme drought conditions in parts of California throughout 2014. The differences arise from different drought indices and precipitation data.

Much of western and central Europe was wet in 2014, but potential ET was also above average over most of Europe. Together these resulted in a complex pattern of drought, with some local severe droughts indicated in parts of central Europe.

Summarizing, the global area under drought conditions was low in 2014. A few regions have seen worsening droughts but drought was alleviated in more regions. Nevertheless, the remarkably small global area with drought conditions contrasts with the high global temperatures for 2014 [see section 2b(1)].

Fig. SB2.4. Mean scPDSI for (upper) 2014 and (lower) the difference between 2014 and 2013. Droughts are indicated by negative values (yellow–red), wet anomalies by positive values (pale–dark blue). No calculation is made where a drought index has no meaning (gray areas: ice sheets or deserts with approximately zero precipitation).

1990–95 protracted El Niño; see Gergis and Fowler 2009).

The SOI trace since 2009 highlights the shift from El Niño to strong La Niña conditions around mid-2010, continuation as a protracted La Niña (with cold SST anomalies in the Niño4 region) until its demise in early 2012 and then near-normal conditions until early 2013. Mainly positive (La Niña-type) values followed until a swing to negative (El Niño-type) conditions since early 2014 (Fig. 2.25b; with warm SST anomalies in the Niño4 region). Major El Niño and La Niña events can be near-global in their influence on world weather patterns, owing to ocean–atmosphere interactions across the Indo–Pacific region with teleconnections to higher latitudes in both hemispheres. Protracted El Niño and La Niña episodes tend to be more regional in their impacts (Allan and D'Arrigo 1999). For example, periods of persistent drought (widespread flooding) in Queensland, Australia, often occur during protracted El Niño (La Niña) episodes. The dry 2014 in much of Queensland (e.g., Plate 2.1 hydrological cycle variables) reflects the marginal El Niño-like conditions.

The SOI is arguably the most global mode of sea level pressure variability. Other regionally notable modes are shown in Fig. 2.25c–j, and illustrate other important characteristics of the circulation. Northern Hemisphere winters (December–February) since 2010/11 have experienced contrasting North Atlantic Oscillation (NAO)/Arctic Oscillation (AO) conditions (Fig. 2.25c,d,g,h). In contrast, in the Southern Hemisphere, the Antarctic Oscillation (AAO) did not exhibit strong features during either of the austral summers of 2013/14 and 2014/15 (Fig. 2.25e,f).